Nuclear Engineering and Technology 57 (2025) 103339

Contents lists available at ScienceDirect

Nuclear Engineering and Technology

journal homepage: www.elsevier.com/locate/net

Original Article

Design and optimization of a source (reflector/shielding) performance test system based on (^{241}Am-Be)-paraffin thermal neutron irradiation device

Nassreldeen A.A. Elsheikh [a,*], I. ElAgib [b], H. AlSewaidan [b], Hamoud A. Kassim [b]

[a] Al-Baha University, Faculty of Science, Department of Physics, P.O. Box 1988, Al-Baha, Saudi Arabia
[b] King Saud University, College of Sciences, Physics & Astronomy Department, P.O. Box 2455, Riyadh, Saudi Arabia

ARTICLE INFO

Keywords:
^{241}Am-Be source
Paraffin moderator
Thermal neutron irradiator
Natural lead
Enriched ^{208}Pb lead

ABSTRACT

Laboratory measurements and Monte Carlo simulations were conducted to investigate the feasibility of employing a (reflector/shield) to improve the efficiency of a thermal neutron irradiator utilizing a paraffin-moderated single ^{241}Am-Be source with an activity of 1 Ci. A multi-parameter optimization was performed to evaluate the potential of natural lead (Pb) and 90 % enriched ^{208}Pb lead (^{208}Pb$_{(90\ \%)}$) in terms of increasing the neutron production while minimizing the total dose equivalent rate. The laboratory-derived optimal configuration for the (reflector/shield) assembly demonstrated that Pb significantly increased the neutron flux by approximately 58 % and reduced the total dose equivalent rate to 0.00443 mSv/h, thereby allowing for a workload of 4500 h within the annual permissible dose limit of 20 mSv. The MCNP simulations validated the potentials of Pb and confirmed the superiority of ^{208}Pb$_{(90\ \%)}$ in terms of increasing neutron flux to about 26 % compared to that measured for Pb, while also minimizing the total dose equivalent rate to 0.0037 mSv/h. Thus, enabling a workload of approximately 5400 h, which is higher by about 20 % compared to that permitted by Pb based on measurements. The geometrical configuration and results promoted the use of the proposed TNI device primarily for prompt gamma neutron activation analysis (PGNAA).

1. Introduction

Thermal Neutron irradiation (TNI) devices are systems combining moderating and shielding materials with neutron sources to get appropriate neutron flux for various irradiation activities ranging from laboratory studies to medical and industrial applications [1–4]. To generate the desired thermal neutron flux, typical fast neutron beams are thermalized by designing an effective beam-shaping assembly (BSA) with an effective moderator that must be designed and configured between the neutron source and the test point [3–6].

Neutron sources include nuclear reactors, neutron generators, and isotope sources [7]. Among these, nuclear reactors and neutron generators are capable of delivering significantly higher neutron fluxes than isotopic sources [7,8]. Nevertheless, the cost of construction and operation of reactors or neutron generators [9], coupled with the short operating lifetime of neutron generators [8], are the main factors limiting their use for in situ and online analysis when compared to the more commonly used isotopic neutron sources such as ^{241}Am-Be and ^{252}Cf [10]. The advantages of these isotopes include their reliable neutron flux, small size, and long half-life [9,11,12]. Moreover, isotopic sources do not necessitate a high-voltage terminal and are of lower cost when compared with research reactors or neutron generators. Consequently, isotopic sources are frequently regarded as viable alternatives for the development of (TNI) facilities, which can be readily integrated into laboratories that do not possess an onsite nuclear reactor or neutron generator, and can be conveniently stored and/or transported between different locations [2,4,13–15].

In this work, ^{241}Am-Be is preferred due to its exceptionally stable flux realized by the long half-life of the ^{241}Am nuclide (432.2 years) compared to that of the ^{252}Cf source (2.645 years) [16]. Furthermore, the ^{241}Am-Be source produces neutrons over an energy range of about (4.14×10^{-7} -11) MeV with an average energy of approximately 4.5 MeV [9,17], while the neutron energy spectrum of ^{252}Cf covers a shorter energy range from about (0.1–6) MeV with lower average neutron energy of about 2.14 MeV [2,8]. Based on these properties of the neutron beam, the ^{241}Am-Be source has long been moderated by paraffin [18], polyethylene [19], or water [12] and employed in the development of TNI facilities that were characterized to meet the requirements of different applications including PGNAA [20], detection of hydrogen in samples [21], detector testing and calibration [19], production of

* Corresponding author.
E-mail address: nelsheikh@bu.edu.sa (N.A.A. Elsheikh).

https://doi.org/10.1016/j.net.2024.11.041
Received 2 September 2024; Received in revised form 13 November 2024; Accepted 24 November 2024
Available online 2 December 2024

radio-elements with short half-lives [12], and neutron shielding performance test [22].

The primary drawback of the ^{241}Am-Be source is its low neutron emission (about 2.2×10^6 n s^{-1} Ci^{-1}) [23], which is obviously several orders of magnitude lower than what can be achieved by nuclear reactors [24] or neutron generators [8]. Therefore, TNI devices based on a^{241}Am-Be source can be effectively used in Prompt Gamma Neutron Activation Analysis (PGNAA) to identify light elements present in bulk samples [25,26]. However, the low thermal neutron flux generated limits the determination of elements present in samples at trace levels to a small number of elements with a sufficiently large cross section [9].

To address such problem, several experimental set-ups and MCNP theoretical models of ^{241}Am-Be-based TNI facilities have been configured using multi-source assemblies [9,11,12,15,27]. This approach can increase the total source intensity and consequently maximize the thermal neutron flux at the test point. In this context, Kotb et al. in Ref. [9] have explored the feasibility of using six identical 5 Ci ^{241}Am-Be sources of 30 Ci total activity and (6.6×10^7 n.s^{-1}) total neutron intensity. In addition, Didi et al. in Ref. [12] have reported the performance of five identical 20 Ci ^{241}Am-Be sources with total activity of 100 Ci and (2.2×10^8 n s^{-1}) total neutron intensity. The results in terms of irradiation performance for the two proposed multi-source TNI assemblies confirmed that the average thermal neutron flux at the test point has increased as the total activity increased, which is an indication of increase in the total neutron intensity of the source assembly.

However, the ^{241}Am-Be source is associated with a significant gamma-ray hazard from the 4.438 MeV γ-rays released by the ^{9}Be(α, n)^{12}C reaction that drives the ^{241}Am-Be source [28]. To evaluate the 4.438 MeV gamma emission for a TNI facility with multiple ^{241}Am-Be sources, one can refer to the ratio of 4.438 MeV gamma to neutron emission ($R=S_\gamma/S_n$) for a single ^{241}Am-Be source, which was measured as ($R = 0.575 \pm 4.8$ %) as reported in Ref. [29]. Applying the average value ($R = 0.575$) together with the neutron emission of about (2.2×10^6 n.s^{-1}.Ci^{-1}) for a single 1 Ci ^{241}Am-Be source, the 4.438 MeV gamma emission ($S_\gamma = R \times S_n$) can be calculated to be about (1.265×10^6 photon.s^{-1}.Ci^{-1}). Consequently, the total 4.438 MeV gamma emission can be calculated to be about (3.795×10^7 photon.s^{-1}) and (1.265×10^8 photon.s^{-1}) for the multi-source geometrical models proposed in Ref. [9] (30 Ci) and [12] (100 Ci), respectively. It can be concluded that the use of a large amount of radioactive material in a multi-source facility leads to significant emissions of 4.438 MeV gamma rays. These emissions contribute to the total dose equivalent rate and thus characterize the optimal operating parameters for the TNI device in accordance with the requirements of the permissible annual dose limit (20 mSv) [30].

In view of such technical challenges, this work investigates the feasibility of using an effective reflecting material around a single ^{241}Am-Be source as an alternative approach to increase the source intensity. This is achieved by reflecting back neutrons scattered away from the moderator upon streaming from the ^{241}Am-Be source. This approach reduces the need for large number of ^{241}Am-Be sources and can therefore enrich the neutron flux at the test point with reduced 4.348 MeV gamma emissions and at affordable operating cost compared with multi-source TNI devices. Furthermore, If the reflecting material is properly selected considering its neutron reflecting and gamma shielding capabilities, it can serve as a dual-purpose (reflector/shield). The dual functionality can effectively minimize the total dose equivalent rate by shielding the 4.438 MeV γ-rays emitted from the ^{241}Am-Be source, thus reducing the need of heavy shielding requirements necessary for multi-source TNI facilities.

A good neutron reflector is characterized primarily by large elastic scattering cross sections and low thermal neutron absorption cross sections [31]. In order to identify an effective method for selecting the optimal reflector, this work introduces neutron reflectivity (R_n) as a measurable parameter that evaluates a material's capability to reflect neutrons. This neutron reflectivity is defined by the ratio of elastic cross section to capture cross section: R_n = (Elastic/Capture). The higher the value of R_n for a material, the greater is its neutron reflecting potentials.

Among several materials, this work compares beryllium (Be) and carbon (C) as elements with low density and low Z-number with lead (Pb) and tungsten (W) as elements with higher density and higher Z-number. To select the most suitable reflector, R_n value for each element was calculated (i) at thermal neutron energy (0.0253 eV) and (ii) over the fission spectrum (10^{-11} - 20 MeV) [32]. The cross section data were taken from Ref. [32] and presented together with the R_n values in Table 1. As shown in Table 1, the results indicate that the R_n values at (0.025 eV) reach a maximum for C (1280) before exhibiting a decline in the following order: Be (766), Pb (74), and W (0.275). This trend can be attributed to the increasing values of the capture cross section. In the context of the fission spectrum, the data shows a peak for Be (2071981) and then follows a similar descending trend as observed at (0.025eV) with C at (102661), Pb at (2348), and W at (92). Notably, the data suggests that lead demonstrates a superior performance compared to tungsten, as evidenced by its higher R_n values at both 0.025 eV and across the fission spectrum.

Based on these facts, beryllium (Be) [2,33] and graphite (C) [34,35] have been widely used as neutron reflectors and have excellent reflective capabilities. Furthermore, results reported in Refs. [36,37] for (Pb) and in Refs. [38,39] for tungsten (W) alloys have shown that both materials also exhibit effective neutron reflection capabilities. Meanwhile, the higher density and atomic number (Z) of Pb (11.34 g cm^{-3}/82) and W (19 g cm^{-3}/74) in comparison to Be (1.85 g cm^{-3}/4) and C (2.26 g cm^{-3}/6) make them suitable alternatives when reflectors with high gamma shielding efficiency are required. This is primarily due to the fact that among the various photon interaction mechanisms, low-energy photons are more effectively absorbed by materials with larger atomic numbers and greater density [40]. However, while the ability of these materials to shield the 4.438 MeV γ-ray emissions associated with the ^{241}Am-Be source is significant, the selection of the most suitable reflector for this work was also determined by its cost. In this regard, despite the higher density of tungsten (19 g cm^{-3}) relative to lead (11.34 g cm^{-3}), lead is favored as a shielding material due to its lower cost and higher atomic number (82) compared to tungsten (74) [4].

On the basis of such considerations, a Pb (reflector/shield) assembly was configured around a single ^{241}Am-Be source and integrated into a laboratory-optimized (^{241}Am-Be)-paraffin TNI facility. The feasibility of the proposed (reflector/shield) was evaluated in terms of improving the neutron production rate in the optimized TNI facility and shielding the 4.438 MeV γ-ray emissions accompanying the ^{241}Am-Be source, thereby reducing the total dose equivalent rate for the operator and surrounding environment.

At this point, it is worth mentioning that paraffin was preferred over polyethylene and water according to the analysis of experimental and MCNP data reported in Refs. [12,41]. In contrast to the MCNP results, the measurements in Ref. [41] showed that paraffin has achieved a more intense moderation effect than polyethylene due to its porosity and has been cited as a better material for neutron shielding. This work uses the inhomogeneous formation of paraffin as a property that enhances the scattering effect, so that fast neutrons could be slowed down over short distances and with few collisions in the moderator [41]. Eventually, this can reduce the volume of the moderator assembly required to achieve higher thermal neutron flux at the test point. On the other hand, the analysis of measurements and MCNP simulations reported in Ref. [12], inferred that paraffin as a moderating material is superior to water, producing a greater thermal neutron flux. In addition, the selection of paraffin was also due to its compatibility with other materials usually used in paraffin moderated TNI devices and that it satisfies their structural requirements [12,15].

However, paraffin generates additional gamma background because fast neutrons can be thermalized to a sufficiently low neutron energy at which they can be easily captured by hydrogen in the paraffin through the ^{1}H(n,γ)^{2}H reaction with a cross section of about (0.3327 b), releasing

Table 1
Cross section data and Reflectivity (R_n) values for Be, C, and natural Pb.

Reaction	Cross sections (barns)							
	Thermal energy (0.0253eV)				Fission spectrum (average)			
	C	Be	Pb	W	Be	C	Pb	W
(n, elastic)	4.942	6.503	11.33	4.988	2.677	2.353	5.624	4.406
(n, γ)	3.86×10^{-3}	8.49×10^{-3}	153.4×10^{-3}	18150×10^{-3}	0.001292×10^{-3}	0.02292×10^{-3}	2.395×10^{-3}	47.64×10^{-3}
Reflectivity (R), rounded off	1280	766	74	0.275	2071981	102661	2348	92

the characteristic 2.223 MeV prompt γ-rays [20]. Such background γ-ray sources also contribute to the total dose equivalent rate and limit the operational lifetime of a TNI device. In view of these prospects, a shielding layer of lead is introduced around the paraffin moderator in this work. In addition to gamma shielding potentials, the lead layer can reduce the neutron losses due to leakage from the moderator and help to collimate neutrons towards the test point.

The laboratory measurements were followed by Monte-Carlo simulations with MCNP5 [42]. The purpose of these simulations was to model and investigate the effectiveness of the proposed Pb (reflector/-shield) in terms of maximizing the neutron flux rates produced by the optimized TNI device model while minimizing the total dose equivalent rate. The MCNP results for Pb were compared with the corresponding measurement data to predict the possible systematic errors so that they can be considered in future applications. On the other hand, additional MCNP simulations were performed to evaluate the performance of $^{208}Pb_{(90\ \%)}$ as a feasible alternative to Pb. This is done by analyzing and comparing the MCNP results for the two materials.

2. Experimental measurements

2.1. Geometrical configuration

The geometrical design consists of ^{241}Am-Be source enclosed in a lead (reflector/shield) and employed in single ^{241}Am-Be-based device for TNI activities. The ^{241}Am-Be fast neutrons were moderated in a lead-shielded paraffin and the (reflector/shield) was optimized to improve the neutron production of the proposed device. The produced neutron flux was measured by a ^{3}He detector enclosed in an external irradiation cavity which was partially shielded by lead. A photograph for the optimal experimental set-up with partially shielded irradiation cavity and the schematic representation of the internal configuration are shown in Fig. 1(a and b).

2.1.1. Neutron source

The ^{241}Am-Be source used in this research was a compact combination of finely powdered AmO_2/Be with a density of 1.3 g cm^{-3}. This mixture was doubly enclosed in a cylindrical stainless-steel capsule, designed mainly to prevent the leakage of radioactive material and increase the durability of the source. The outer dimensions of the capsule were 5 cm length and 3 cm diameter. The total activity of the ^{241}Am-Be source was 1 Ci with an intensity of about (2.2×10^6 n.s^{-1}) [43]. When the source was not in use, it was stored in a lead-shielded container filled with paraffin wax. This serves to absorb the possibly escaping thermalized neutrons and shield the potential gamma emissions, primarily the 4.438 MeV γ-rays that accompany the ^{241}Am-Be source. During irradiation, the source was fitted in a source holder and actively moved from the storage facility to the experimental site where the TNI device was configured. The source was then precisely inserted at the irradiation position of the proposed (reflector/shield) assembly. The TNI device was configured on a laboratory bench 100 cm horizontally from the storage facility and 115 cm above the laboratory floor.

2.1.2. (Reflector/shield)

The ^{241}Am-Be source was inserted into a cylindrical cavity with a diameter of 3.5 cm and a length of 9 cm, which was drilled around the central x-axis of a rectangular lead structure measuring 30 cm length, 9 cm width and 25 cm height. In order to direct the neutrons from the source and enhance their flow towards the irradiation cavity, the source was positioned on the x-axis with the head of the source at 4 cm away

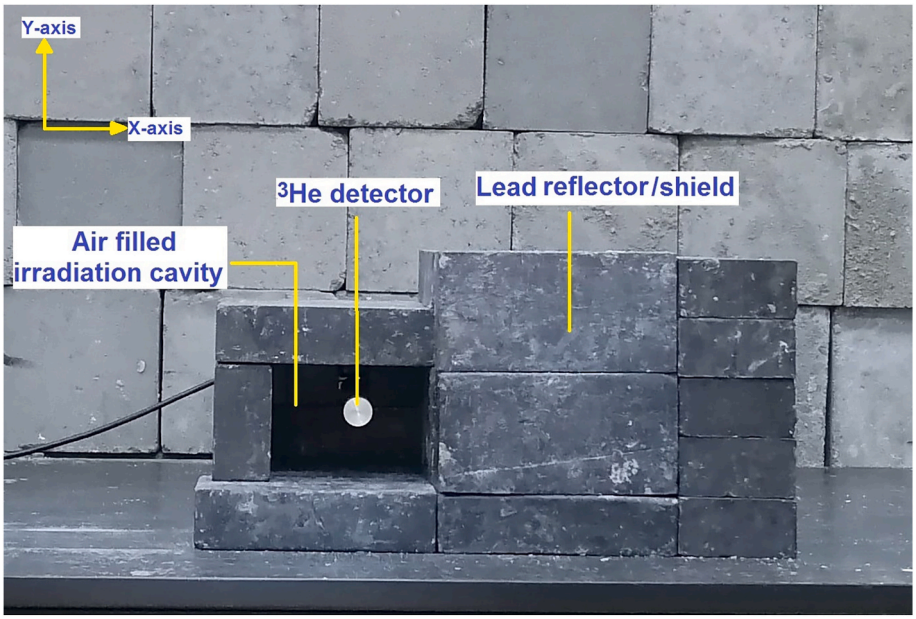

Fig. 1 (a). A photograph for the optimal experimental set-up.

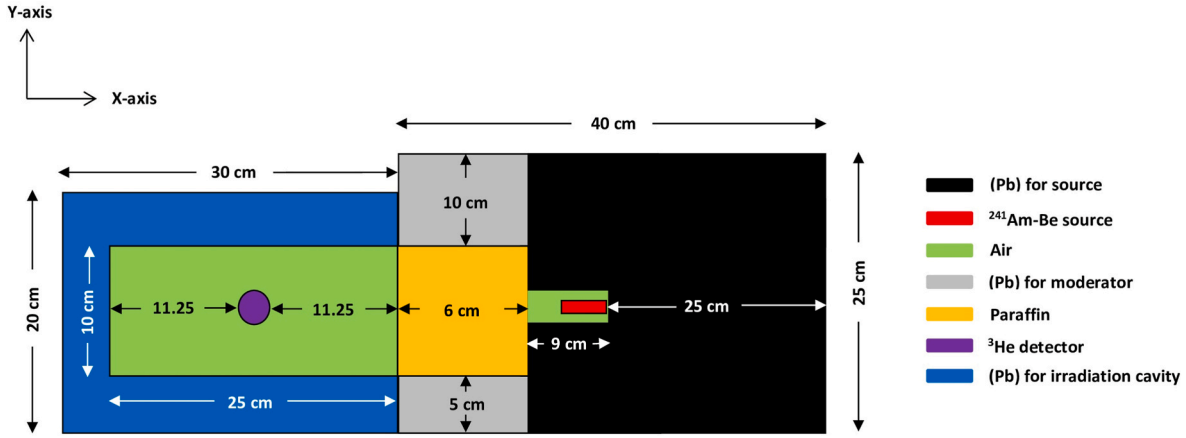

Fig. 1 (b). Schematic representation of the internal device configuration.

from the moderator entrance port. The dimensions of the lead assembly containing the source were kept constant, while the length of its extension behind the source was varied and referred to as the (reflector/shield) thickness in the laboratory measurements and MCNP simulations. It is important to note that the lead assembly consists of Pb bricks with dimensions of 30 cm length, 10 cm width and 5 cm thickness.

2.1.3. Moderator

Paraffin with density (0.93 g cm^{-3}) was selected as the fast neutron moderator for the current measurements. The moderator assembly was configured as rectangular volume consisted of paraffin slabs, each measuring 30 cm in length, 10 cm in width, and 3 cm in thickness. A layer of lead, 5 cm thick at the bottom and sides, and 10 cm thick on top, was used to partially shield the moderator assembly, leaving the entry and exit ports unshielded.

2.1.4. Thermal neutron detector

The ^{3}He proportional counter LND.INC-252, with an effective length of 20.3 cm and diameter of 2.5 cm, was utilized as the detector in this study. In comparison to other thermal neutron detectors like $^{10}BF_3$ and ^{6}Li, the thermal neutron absorption cross section for the $^{3}He(n,p)^{3}H$ reaction (5330 b) is higher than that of $^{10}B(n,\alpha)^{7}Li$ (3840 b) and $^{6}Li(n,\alpha)^{3}H$ (940.983 b) by factors of about 1.4 and 5.7, respectively [8,44].

This difference in cross sections results in a higher efficiency of ^{3}He detectors when compared to $^{10}BF_3$ and ^{6}Li detectors. Therefore, the selection of a ^{3}He detector is a reasonable choice for the current ^{241}Am-Be-based TNI. The ^{3}He detector was positioned on the central z-axis of a rectangular irradiation cavity of dimensions 25 cm width, 30 cm length, and 10 cm height, with its effective length perpendicular to the direction of the neutrons coming from the moderator. It should be noted that the irradiation cavity was shielded with a 5 cm thick (Pb) layer, primarily to reflect back the neutrons entering the cavity and scattered away from the ^{3}He detector. On the other hand, it is important to emphasize that the measurements were performed with an acquisition time of 300s per control.

3. Experimental results

3.1. Moderator optimization

The measurements were started at a (reflector/shield) thickness of 0 cm. The ^{3}He counts (I) were then measured while the ^{241}Am-Be source remained in position, and the paraffin thickness was incrementally increased in 3 cm intervals within the range of (0–15) cm. To determine the net counts at each thickness interval, the neutron background counts (I_o) were measured without ^{241}Am-Be source in place and subsequently subtracted from (I). The signals generated by the ^{3}He detector were processed through an amplifier-discriminator unit, with the filtered pulse height being transmitted to a multi-channel analyzer connected to a desktop computer.

The results were analyzed in terms of changes in the net counts ($I-I_o$) as a function of paraffin thickness and presented in Fig. 2. It is important to note that only superimposed curves representing the best fit to the data were presented during both laboratory measurements and MCNP calculations. As shown in Fig. 2, the ^{3}He counts increase with the moderator thickness from (0–6), peaking at approximately (1.11×10^{5} counts.s^{-1}) at a thickness of 6 cm.

This increase is primarily due to the energy loss of neutrons through elastic collisions with hydrogen atoms present in the paraffin. However, as the thickness further increases from (9–15) c m, the net counts decrease due to the absorption of thermalized neutrons in the expanding volume of the moderator through the $^{1}H(n,\gamma)^{2}H$ reaction. Thus, a thickness of 6 cm was determined to be the optimal moderator thickness.

3.2. Reflector optimization

The moderator thickness was set to (6 cm) and the corresponding highest counts (1.11×10^{5} counts.s^{-1}) were given the symbol (I_{mod}) and maximized by increasing the (reflector/shield) thickness in increments of 5 cm over a range of (0–25) cm. The background-subtracted ^{3}He counts were recorded at each thickness increase and labeled with the symbol ($I_{(ref/shi)}$). The results were analyzed in terms of the variations of net counts [$I_{(ref/shi)}$-I_{mod}] with the thickness of the (reflector/shield) and plotted in Fig. 3. As can be seen in Fig. 3, the net counts increase rapidly with increasing thickness in the range of (0–10 cm), which can be

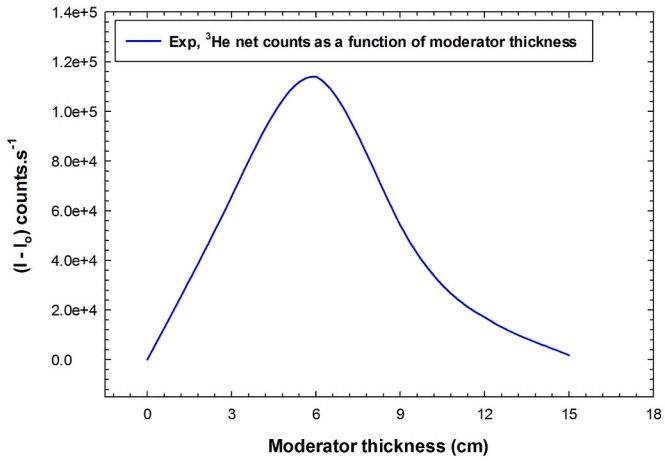

Fig. 2. Measured ($I-I_o$) counts as a function of moderator thickness.

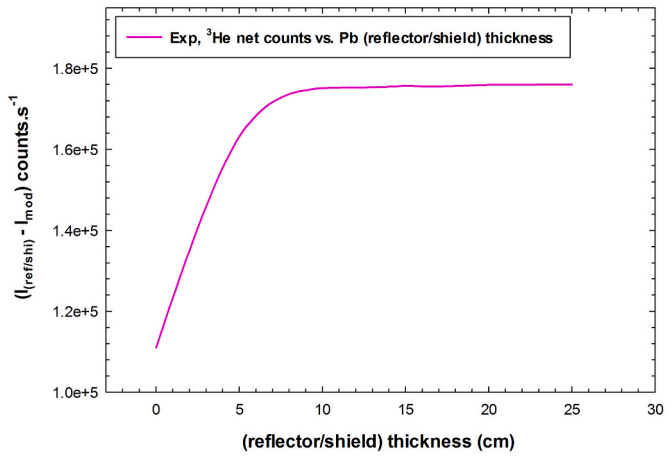

Fig. 3. Measured ($I_{(ref/shi)}$- I_{mod}) counts as a function of Pb (reflector/shield) thickness.

attributed to the increase in $I_{(ref/shi)}$ counts within this thickness range. However, a stepwise increase in net counts was observed at further thickness increments of (15–25 cm), with the highest counts (1.76×10^5 counts.s^{-1}) measured at 25 cm, which was considered to be the optimal thickness.

This trend can be attributed to the decrease in $I_{(ref/shi)}$ signals with increasing thickness. On the one hand, this could be explained by the fact that lead is a competitive neutron shielding material [45]. Given the steps of the ideal shielding process described in Ref. [45], the fast neutrons are rapidly reduced in energy by inelastic scattering processes, then decelerated into thermal neutrons by several elastic scattering processes, and finally absorbed into Pb by (n,γ) capture reactions. On the other hand, the moderated neutrons, which may have been scattered back into the paraffin moderator as $I_{(ref/shi)}$ signals, are further slowed down enough to be captured by the $^1H(n,\gamma)^2H$ reactions before reaching the ^{3}He detector.

At this point, the optimal (reflector/shield) dimensions were set at 34 cm in length, 30 cm in width and 25 in height. As a result, the physical dimensions of the (^{241}Am-Be)-paraffin configuration (excluding the irradiation cavity) were determined to be 40 cm in length, 30 cm in width and 25 in height. The results showed that the proposed (reflector/shield) configuration effectively increased the ^{3}He counts measured for I_{mod} (1.11×10^5 counts.s^{-1}) by about 58 %.

On the other hand, the results indicated that when the proposed TNI device is considered as a thermal neutron probe for PGNAA, the sample at the test point could receive about 8 % of the neutron source intensity (2.2×10^6 n.s^{-1}) compared to about 5 % produced without the use of the proposed (reflector/shield).

The cost analysis indicated that the weight of the lead (Pb) used for the (reflector/shield) configuration was approximately 288.2 kg, excluding the air-filled cylindrical cavity that houses the source. Additionally, the weight of the lead that shields the paraffin moderator was estimated to be around 37.4 kg. Given that the price of lead is set at 2 USD per kilogram, the total cost for the lead material (325.6 Kg) was calculated to be 651.2 USD. Conversely, the weight of the paraffin was determined to be about 1.67 kg, and with a price of 1.66 USD per kilogram, the expense for the paraffin was around 2.8 USD. Consequently, the combined material costs totaled 654 USD. Considering these material prices, the overall estimated cost for the proposed (^{241}Am-Be)-paraffin test system (excluding the costs of the lead that shields the irradiation cavity and the ^{3}He detector contained within it), was projected to range between 10654 and 20654 USD, contingent upon the estimated price for a 1 Ci ^{241}Am-Be source.

3.3. Measurement of dose equivalent rates

The total gamma dose equivalent rate ($D\gamma_{(T)}$) including the doses resulted from the γ-ray emissions produced by the (n,γ) reactions within the moderator and (reflector/shield) assembly, as well as the primary γ-rays from the ^{241}Am-Be source, was measured at a distance of 100 cm from the (^{241}Am-Be)-paraffin assembly while varying the thickness of the (reflector/shield) by 5 cm increments over a range of 0–25 cm. These measurements were taken using a Fluke 451P-DE-SI dose rate probe and the results were analyzed in terms of variations in $D\gamma_{(T)}$ values with increasing (reflector/shield) thickness and reported in Fig. 4. As observed in Fig. 4, the results showed that the $D\gamma_{(T)}$ values decreased as the thickness increased, with the lowest value measured as about (0.0025 mSv/h) at a thickness of 25 cm. This result reconfirms the use of 25 cm as the optimal thickness. At this thickness, the neutron dose equivalent rate $D_{(n)}$ was measured as about (0.00193 mSv/h) using a Berthold LB 6411 dose rate probe. Consequently, the total dose equivalent rate [$D_{(T)} = D\gamma_{(T)} + D_{(n)}$] was calculated as about (0.00443 mSv/h).

As a result, if the proposed (^{241}Am-Be)-paraffin TNI device is operated for1000 h/year, a total dose of 4.43 mSv is expected, which corresponds to an operational duration of about 4500 h within the requirements of the annual permissible dose limit. In contrast, the measured dose rate D_T (0.031 mSv/h) at a fixed (reflector/shield) thickness of 0 cm indicates that the operational time is limited to approximately 645 h before reaching the permissible dose limit. These findings demonstrate that the use of Pb has significantly decreased the total dose rate and extended the operational time by a factor of roughly 7.

4. MCNP modeling

The results from the laboratory-optimized (reflector/shield) indicated that the use of Pb effectively increased the ^{3}He counts by about 58 % and decreased the radiological doses D_T by a factor of 3. This comparison was made against the I_{mod} and D_T values achieved by the (^{241}Am-Be)-paraffin device, with the thickness of the (reflector/shield) assembly maintained at 0 cm.

The effective reflective potentials of natural Pb have been mainly attributed to the presence of ^{208}Pb isotope, which exhibits the highest reflectivity (R_n) among its main constituent isotopes, characterized by their respective abundances: ^{208}Pb (52 %), ^{206}Pb (24 %), ^{207}Pb (23 %) and ^{204}Pb (1 %) [46]. To verify this, the R_n values for the four isotopes of Pb were determined at thermal neutron energy (0.025 eV) and across the fission spectrum, utilizing the cross section data provided in Ref. [32]

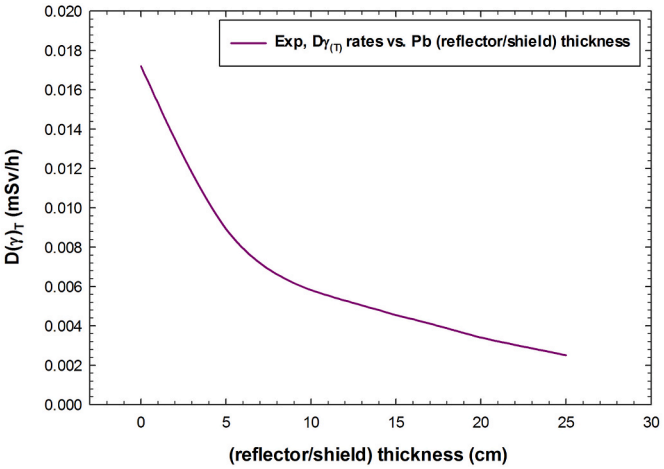

Fig. 4. Measured total gamma dose equivalent rates ($D\gamma_{(T)}$) as a function of Pb (reflector/shield) thickness.

and summarized in Table 2. The results presented in Table 2 confirmed the superiority of ^{208}Pb in terms of reflectivity at both (0.025 eV) and across the fission spectrum when compared to the other isotopes of Pb.

On the other hand, a comparison with the results for natural Pb presented in Table 1 reveals that at thermal neutron energy (0.0253 eV), the capture cross section of ^{208}Pb (0.5009×10^{-3} b) is significantly lower than that of Pb (153.4×10^{-3} b) by a factor of about 306 [32]. In contrast, the elastic scattering cross sections of ^{208}Pb (11.5 b) and Pb (11.33b) do not differ significantly [32]. However, the reduced capture cross section of ^{208}Pb resulted in a reflectivity value of about (22959), which is a factor of about 310 higher than that of Pb (74). Furthermore, when examining the average capture cross section of ^{208}Pb (1.437×10^{-3} b) across the fission spectrum, it is found to be lower than that of Pb (2.395×10^{-3} b) by a factor of roughly 1.7. However, the average elastic scattering cross sections for ^{208}Pb (6.097 b) and Pb (5.624 b) do not show significant differences [32]. Nonetheless, the lower average capture cross section of ^{208}Pb resulted in a reflectivity value of about (4243), which is a factor of about 1.8 higher than that of Pb (2348).

Therefore, the use of lead with predominant content of ^{208}Pb has the potential to improve the efficiency of the laboratory-optimized Pb (reflector/shield), thereby maximizing the ^{3}He counts at the test point of the proposed TNI device. Natural Pb can be enriched to 99.0 % ^{208}Pb by gas centrifugation, as indicated in Ref. [47], with associated costs estimated between 1000 and 2000 USD per kilogram. In contrast, it can be extracted at a significantly lower cost from aged thorium ore with 85–93 % enrichment of ^{208}Pb, depending on the quality of the ore [47]. In this regard, the research cited in Ref. [48] determined that the hydrometallurgical extraction of Pb with high ^{208}Pb enrichment from monazite (the primary thorium ore) is projected to cost between 24 and 30 USD per kilogram. However, to maintain affordability in future models, this study explores the viability of using Pb enriched to 90 % ^{208}Pb, characterized by an isotopic composition of ^{208}Pb (90 %), ^{206}Pb (9 %), ^{207}Pb (0.8 %), and ^{204}Pb (0.2 %).

4.1. Geometry characterization

The source was modeled as a volume source enclosed in a cylindrical stainless steel with dimensions similar to those used for measurements and given the neutron energy distribution characteristic of a^{241}Am-Be source producing (2.2×10^{6} n.s^{-1}). The simulated stainless steel was of density (7.93 g cm^{-3}) and elemental mass fractions of: C(0.004 %), Si (0.37 %), P(0.011 %), S(0.008 %), Cr(16.96 %), Mn (1.59 %), Fe(65.157 %), Ni(13.61 %), and Mo(2.29 %). The uniform particle position sampling was given by the (EXT) variable. While for the source radius values (RAD), a power law built-in function $p(x) = c|x|^{a}$ was used with $a = 1$.

The measured and normalized neutron spectra of ^{241}Am-Be source were taken from Ref. [20], while the spectra of the accompanying γ-rays were generated by multiplying the measured γ-ray spectrum (per emitted neutron) from Ref. [21] by the intensity of the actual ^{241}Am-Be source. The calculations were performed with up to 10^{7} histories within the same acquisition time (300s) of the laboratory measurements and the cross sections were derived from the ENDF/B-VI, and the NJOY libraries. These parameters ensured a sufficient number of histories resulting in a statistically acceptable MCNP error of less than 0.03 %.

The (reflector/shield) was modeled as a rectangular volume with dimensions matching those of the actual measurements. The source was located inside an air-filled cylindrical cavity, which was modeled around the central x-axis of the (reflector/shield) assembly, with dimensions comparable to measurements. The source was positioned at the entrance of the moderator which was simulated as a rectangular volume filled with paraffin and partially shielded with lead. The moderator dimensions and thickness of the lead layer were corresponded to those of measurements.

The ^{3}He detector was modeled with similar dimensions used in the experimental work and centered on the z-axis of the irradiation cavity which was air-filled and shielded with lead. The dimensions of the cavity and the thickness of the lead shielding were consisted with those employed in the measurements. The detector was aligned perpendicular to the direction of the incoming neutron beam and the flux-over-cell tally (F4) was used to exclusively record the thermal neutron counts detected by the ^{3}He(n,p)^{3}H reaction. The elemental compositions and densities of Pb, $^{208}Pb_{(90\ \%)}$, AmO_2/Be mixture, paraffin, and air as modeled in the MCNP simulations are provided in Table 3.

5. MCNP results

The MCNP calculations were performed following the same methodology used for the measurements. Initially, the thickness of the (reflector/shield) was fixed at 0 cm and the ^{3}He net count rates ($I - I_o$) were calculated with increasing moderator thickness in 3 cm increments and over the thickness range (0–15) cm considered for the measurements. Similar to the measurements, the highest ^{3}He count rates (I_{mod}) were observed at the optimal moderator thickness (6 cm) and determined to be approximately (1.14×10^{5} counts.s^{-1}). The (reflector/shield) volume housing the source was alternately filled with Pb and $^{208}Pb_{(90\ \%)}$, and the net counts ($I_{(ref/shi)} - I_{mod}$) were determined while the (reflector/shield) thickness was incrementally increased by 5 cm within the range of (0–25) cm considered for the measurements. The MCNP results were compared with the measurement results for Pb and are presented in Fig. 5. Similar to the trend observed in Figs. 3 and 5 shows that the net signals increased rapidly in the range of (0–10) cm and peaked at a thickness of 10 cm. As the thickness increased from 15 cm to 25 cm, the net counts progressively increased due to the decrease in $I_{(ref/shi)}$ signals, with the highest net counts of about (1.82×10^{5} counts.s^{-1}) and (2.21×10^{5} counts.s^{-1}) recorded at 25 cm thickness for the simulated Pb and $^{208}Pb_{(90\ \%)}$, respectively.

It was observed in Fig. 5 that the highest MCNP value determined for Pb was approximately 3 % higher than the corresponding measured value (1.76×10^{5} counts.s^{-1}). The primary cause of this could be the fast neutron response of a physical ^{3}He detector that limits the counting rate at which the detector can be operated. This is realized by the considerable sensitivity estimated on the scale of 10^{-3} that physical thermal neutron detectors such as ^{3}He detectors, exhibit in response to fast neutrons (up to $E_n = 10$ MeV) [8,49]. Therefore, such systematic error should be taken into accounts when operating the proposed TNI device as a monitoring system for thermal neutrons. In this context, ^{3}He tubes are usually embedded inside a solid polyethylene moderator in order to optimize the moderation effect [50,51]. On the other hand, cadmium has been employed at different response tuning assemblies to increase the ^{3}He sensitivity for thermal neutrons and consequently improve its

Table 2
Cross section data and reflectivity (R_n) values for^{208}Pb,^{207}Pb,^{206}Pb, and^{204}Pb.

Reaction	Cross sections (barns)							
	Thermal energy (0.0253eV)				Fission spectrum (average)			
	^{208}Pb	^{206}Pb	^{207}Pb	^{204}Pb	^{208}Pb	^{207}Pb	^{206}Pb	^{204}Pb
(n, elastic)	11.50	10.85	11.51	12.23	6.097	5.380	5.020	5.011
(n, γ)	0.5009×10^{-3}	26.56×10^{-3}	610.1×10^{-3}	703.2×10^{-3}	1.437×10^{-3}	2.804×10^{-3}	3.939×10^{-3}	32.83×10^{-3}
Reflectivity (R), rounded off	22959	409	19	17	4243	1919	1274	153

Table 3
Compositions and densities of AmO_2/Be mixture, Pb, $^{208}Pb_{(90\ \%)}$, paraffin, and air, as modeled in the MCNP simulations (rounded off).

Material	Density g.cm^{-3}	Mass fractions									
		H	Be	C	N	O	Am	^{208}Pb	^{207}Pb	^{206}Pb	^{204}Pb
AmO_2/Be	1.3		0.994		0.004	0.002					
Pb	11.34							0.52	0.23	0.24	0.01
$^{208}Pb_{(90\ \%)}$	11.34							0.90	0.09	0.008	0.002
Paraffin	0.93	0.149		0.851							
Air	0.00122				0.780	0.220					

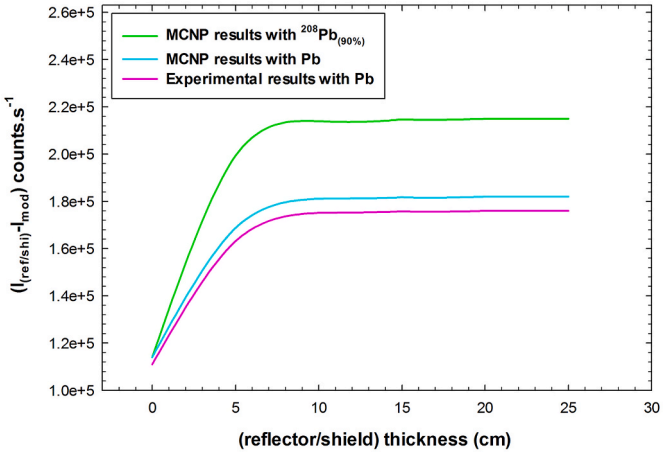

Fig. 5. MCNP ($I_{(ref/shi)}$- I_{mod}) counts as a function of $^{208}Pb_{(90\ \%)}$ (reflector/shield) thickness plotted against the corresponding MCNP and measured data for Pb.

detection efficiency [22].

The MCNP data in Fig. 5 also showed that the highest ^{3}He counts for $^{208}Pb_{(90\ \%)}$ (2.21×10^5) exceeds those achieved by Pb in MCNP simulations (1.82×10^5) and measurements (1.76×10^5) by about 21 % and 26 %, respectively. As a consequent, the use of $^{208}Pb_{(90\ \%)}$ has effectively increased the neutron counts at the test point to about 10 % of the neutron source intensity compared to about 8 % for Pb according to both MCNP and measurements data.

5.1. Calculation of dose equivalent rates

The total dose equivalent rate $D_{(T)}$ was derived in a manner similar to the measurements and determined in (mSv/h) at a distance of 100 cm from the optimal MCNP model. However, the constituent doses of $D\gamma_{(T)}$ resulting from the secondary γ-rays ($D\gamma_{(Sec)}$) and the primary γ-ray flux ($D\gamma_{(source)}$) were calculated separately when the source was simulated solely with neutron or gamma spectra, respectively. Subsequently, the total gamma dose equivalent rate was determined as ($D\gamma_{(T)} = D\gamma_{(Sec)} + D\gamma_{(source)}$) and added to the neutron dose equivalent rate D_n. It is worth noting that the flux tally at a point (F5) was used to determine the normalized source fluxes, which were then converted to dose equivalent rates by using the MCNP5 dose energy (DE) and dose function (DF) flux-to-dose conversion factors. Considering this procedure, the total dose equivalent rate (D_T) was calculated as about (0.0037 mSv/h). Consequently, operating the (^{241}Am-Be)-paraffin model for1000 h/year would results in a neutron dose of 3.7 mSv, indicating that the MCNP model could function for roughly 5400 h while adhering to the annual permissible dose limit.

In comparison to the laboratory-derived (D_T) value (0.00443 mSv), the MCNP model has predicted an operating time that is higher by about 20 %. However, it is imperative to consider these findings in light of the neutron and gamma background counts during measurements, the uncertainties in the material composition, and the statistical errors in the MCNP results which were noted to be around 0.03 %.

6. Conclusion

The current study involved comparative measurements and MCNP optimizations performed to evaluate the potential of a Pb (reflector/shield) assembly as an alternative approach to improve the neutron production of a single (^{241}Am-Be)-paraffin TNI device with reasonable minimum radiological doses. Further MCNP simulations were performed to explore the use of $^{208}Pb_{(90\ \%)}$ as a potential replacement for Pb.

The optimal dimensions of Pb (reflector/shield) were determined by measuring 34 cm in length, 30 cm in width, and 25 cm in height, and the results showed that Pb effectively increased the ^{3}He counts by approximately 58 % at a reasonably low dose rate (D_T) of approximately (0.00443 mSV/h), permitting approximately 4500 h of operation without exceeding the annual dose limit. The estimated cost of the integrated (^{241}Am-Be)-paraffin test system (40 cm × 30 cm × 25 cm) was estimated at a range of 10654–20654 USD.

The MCNP model for the Pb (reflector/shield) with optimal configuration validated the laboratory-optimized design, revealing that the highest predicted ^{3}He count was approximately 3 % higher than that obtained in the measurements. In contrast, replacing Pb with $^{208}Pb_{(90\ \%)}$ resulted in a significant increase in both predicted and measured ^{3}He counts, with enhancement of approximately 21 % and 26 %, respectively. The use of $^{208}Pb_{(90\ \%)}$ also lead to an increase in neutron counts at the test point, reaching about 10 % of the neutron source intensity, compared to around 8 % generated by Pb, as indicated by both the MCNP simulations and experimental data. Furthermore, the dose rate (D_T) associated with $^{208}Pb_{(90\ \%)}$ was estimated to be approximately 0.0037 mSv/h, which is about 16 % lower than the corresponding value for Pb derived from measurements. This reduction allows for an operational duration of approximately 5400 h, representing an increase of about 20 % compared to the duration permitted by Pb.

These findings suggest the use of $^{208}Pb_{(90\ \%)}$ as a viable replacement for the natural Pb, thereby confirming its applicability in the proposed (reflector/shield) configuration to increase the intensity of the ^{241}Am-Be source and subsequently improve neutron production in the proposed (^{241}Am-Be)-paraffin TNI, while maintaining a relatively low dose equivalent rate. However, the use of $^{208}Pb_{(90\ \%)}$ may lead to a considerable increase in costs. Nevertheless, its use is justified based on the results obtained and the capabilities of the current TNI device.

The results imply that the device can be effectively utilized as a thermal neutron probe for Prompt Gamma Neutron Activation Analysis (PGNAA) conducted outside a nuclear reactor. This capability ensures reliable flux intensity at the measurement location while remaining cost effective. Moreover, the device is also capable of operating as a neutron spectrometer for hydrogen detection. Furthermore, the generated neutron flux can be used for testing and calibrating thermal neutron detectors such as ^{3}He, particularly in relation to their detection efficiency.

CRediT authorship contribution statement

Nassreldeen A.A. Elsheikh: Writing – original draft, Supervision,

Software, Methodology, Investigation. **I. ElAgib:** Validation, Conceptualization. **H. AlSewaidan:** Formal analysis. **Hamoud A. Kassim:** Resources, Data curation.

Declaration of competing interest

The authors declare that they have no known competing financial interests or personal relationships that could have appeared to influence the work reported in this paper.

Acknowledgement

The authors wish to extend their gratitude to the Department of Physics within the Faculty of Science at Al-Baha University, as well as to the Physics& Astronomy Department at the College of Sciences, King Saud University, for their generous provision of necessary facilities.

References

[1] J. Rataj, P. Suk, T. Bílý, M. Štefánik, J. Frýbort, Characterisation of neutron field in the polyethylene neutron irradiator, Appl. Radiat. Isot. 168 (2021) 109529.
[2] N.A.A. Elsheikh, Characterization of (^{252}Cf-ZrH_2) Monte Carlo model for detection of nitrogen and chlorine by thermal neutron-capture PGNAA, Radiat. Phys. Chem. 188 (2021) 109591.
[3] A. Waheed, N. Ali, M.A. Baloch, A.A. Qureshi, E.A. Munem, M.U. Rajput, T. Jamal, W. Muhammad, Optimization of moderator assembly for neutron flux measurement: experimental and theoretical approaches, Nucl. Sci. Tech. 28 (2017) 28–61.
[4] N.A.A. Elsheikh, Monte Carlo modelling of a neutron-induced gamma-ray sensor for landmine or explosive detection, Journal of Radiation Research and Applied Sciences 11 (2018) 403–407.
[5] E. Bavarnegin, Y. Kasesaz, F.M. Wagner, Neutron beams implemented at nuclear research reactors for BNCT, J. Instrum. 12 (2017). P05005-P05005.
[6] F. Rahmani, M. Shahriari, Beam shaping assembly optimization of linac based BNCT and in-phantom depth dose distribution analysis of brain tumors for verification of a beam model, Ann. Nucl. Energy 38 (2011) 404–409.
[7] J.Y. Zevallos, C.B. Zamboni, Evaluation of the neutron flux distribution in an AmBe Irradiator using the MCNP-4C code, Braz. J. Phys. 35 (3b) (2005) 797–800.
[8] N.A.A. Elsheikh, Comparative optimization of Be/Zr$(BH_4)_4$ and Be/Be$(BH_4)_2$ as ^{252}Cf source shielding assemblies: effect on landmine detection by neutron backscattering technique, Nucl. Eng. Technol. 54 (2022) 2614–2624.
[9] N.A. Kotb, A.H.M. Solieman, T. El-Zakla, T.Z. Amer, S. Elmeniawi, M.N.H. Comsan, Multi-source irradiation facility with improved space configuration for neutron activation analysis: design optimization, Appl. Radiat. Isot. 135 (2018) 135–141.
[10] J. Rusnak, Z. Vykydal, Determination of a Pu-Be source neutron spectrum at Czech Metrology Institute, Appl. Radiat. Isot. 175 (2021) 109786.
[11] Z. Idiri, H. Mazrou, A. Amokrane, S. Bedek, Characterization of an Am-Be PGNAA set-up developed for in situ liquid analysis: application to domestic waste water and industrial liquid effluents analysis, Nucl. Instrum. Methods Phys. Res. B 268 (2010) 213–218.
[12] A. Didi, A. Dadouch, O. Jaï, J. Tajmouati, H. El Bekkouri, Neutron activation analysis: modelling studies to improve the neutron flux of Americium Beryllium source, Nucl. Eng. Technol. 49 (2017) 787–791.
[13] L. Yongsheng, J. Wenbao, H. Daqian, S. Qing, C. Can, Z. Haojia, et al., A new Am-Be PGNAA setup for element determination in aqueous solution, Appl. Radiat. Isot. 95 (2015) 233–238.
[14] N.H. Moadab, M.K. Saadi, Optimization of an Am-Be neutron source shield design by advanced materials using MCNP code, Radiat. Phys. Chem. 158 (2019) 109–114.
[15] D. Meena, S.K. Gupta, H.S. Palsania, N. Jakhar, N. Chejara, P. Meena, Characterization of Am-Be neutron source based PGNAA setup using aqueous solutions of Chlorine and Boron, International Journal of Radiation Research 17 (2019) 301–308.
[16] M. Asamoah, B.J.B. Nyarko, J.J. Fletcher, R.B.M. Sogbadji, S. Yamoah, S. E. Agbemava, E. Mensimah, Neutron flux distribution in the irradiation channels of Am-Be neutron source irradiation facility, Ann. Nucl. Energy 38 (2011) 1219–1224.
[17] N.A.A. Elsheikh, Multi-parameter optimization of a (^{3}He-^{252}Cf-^{3}He) neutron backscattering sensor for landmine detection, Journal of Radiation Research and Applied Sciences 10 (2017) 122–127.
[18] A. Waheed, N. Ali, M.A. Baloch, A.A. Qureshi, E.A. Munem, M.U. Rajput, T. Jamal, W. Muhammad, Optimization of moderator assembly for neutron flux measurement: experimental and theoretical approaches, Nucl. Sci. Tech. 28 (2017) 61.
[19] R. Bedogni, D. Sacco, J.M. Gómez, M. Lorenzoli, A. Gentile, B. Buonomo, A. Pola, M.V. Introini, D. Bortot, C. Domingo, ETHERNES: a new design of radionuclide source-based thermal neutron facility with large homogeneity area, Appl. Radiat. Isot. 107 (2016) 171–176.
[20] L.E. Cevallos, G.F. García, A. Lorente, E. Gallego, H.R. Vega, K.A. Guzmán, Design by Monte Carlo method of a thermal neutron device using a ^{241}Am/^{9}Be source and high-density polyethylene moderator, Appl. Radiat. Isot. 151 (2019) 150–156.
[21] S.A. Jonah, I.I. Zakari, S.B. Elegba, Determination of the hydrogen content of oil samples from Nigeria using an Am–Be neutron source, Appl. Radiat. Isot. 50 (1999) 981–983.
[22] D. Zhao, W. Jia, D. Hei, C. Cheng, J. Li, P. Cai, Y. Chen, Design of a neutron shielding performance test system base on Am-Be neutron source, Radiat. Phys. Chem. 193 (2022) 109954.
[23] E. Mensimah, R.G. Abrefah, B.J.B. Nyarko, J.J. Fletcher, M. Asamoah, Neutron flux determination in irradiation sites of an Am-Be neutron source at NNRI, Ann. Nucl. Energy 38 (2011) 2303–2308.
[24] C. Stasser, G. Terwagne, J. Lamblin, O. Méplan, G. Pignol, B. Coupé, S. Kalcheva, S. Van Dyck, M. Sarrazin, Probing neutron-hidden neutron transitions with the MURMUR experiment, Eur. Phys. J. C 81 (2021) 17.
[25] M.A.A. Mandour, A. Badawi, N.M.A. Mohamed, A. Emam, Towards a methodology for bulk sample neutron activation analysis, J. Taibah Univ. Sci. 10 (2016) 235–241.
[26] J.G. Fantidis, G.E. Nicolaou, C. Potolias, N. Vordos, D.V. Bandekas, The comparison of four neutron sources for Prompt Gamma Neutron Activation Analysis (PGNAA) in vivo detections of boron, J. Radioanal. Nucl. Chem. 290 (2011) 289–295.
[27] K. Tuffour, B.J.B. Nyarko, E.H.K. Akaho, M. Asamoah, R.M.B. Sogbadji, R. G. Abrefah, J. Boffie, Re- design of ^{241}Am–Be neutron source irradiator facility at NNRI using MCNP-5 code, Ann. Nucl. Energy 40 (2012) 60–64.
[28] H.M. Hakimabad, H. Panjeh, A.V. Noghreiyan, Shielding studies on a total-body neutron activation facility, Iran. J. Radiat. Res. 5 (1) (2007) 45–51.
[29] Z. Liu, J. Chen, P. Zhu, Y. Li, G. Zhang, The 4.438 MeV gamma to neutron ratio for the Am–Be neutron source, Appl. Radiat. Isot. 65 (2007) 1318–1321.
[30] C.P. Datema, V.R. Bom, C.W.E. Van Eijk, Experimental results and Monte Carlo simulations of a landmine localization device using the neutron backscattering method, Nucl. Instrum. Methods 488 (2002) 441–450.
[31] D. Blanchet, B. Fontaine, Reflector and protections in a Sodium-cooled fast reactor: modelling and optimization, EPJ Web Conf. 153 (2017) 05006.
[32] JAEA Nuclear Data Center: https://wwwndc.jaea.go.jp/.
[33] H. Basiri, H.T. Anbaran, Investigation of some possible changes in Am-Be neutron source configuration in order to increase the thermal neutron flux using Monte Carlo code, J. Phys. Conf. 956 (2018) 012010.
[34] S. Azimkhani, F. Zolfagharpour, F. Ziaie, Investigation of reflection properties of applied reflectors for thermal neutrons by considering the albedo and spectral shift, Prog. Nucl. Energy 100 (2017) 192–196.
[35] M. Albarhoum, Graphite reflecting characteristics and shielding factors for miniature neutron source reactors, Ann. Nucl. Energy 38 (2011) 14–20.
[36] A.A. Burlon, A.J. Kreiner, A.A. Valda, D.M. Minsky, An optimized neutron-beam shaping assembly for accelerator-based BNCT, Appl. Radiat. Isot. 61 (2004) 811–815.
[37] A.A. Burlon, A.J. Kreiner, S.M. White, B.W. Blackburn, D.P. Gierga, J.C. Yanch, Phantom dosimetry for the ^{13}C(d,n)^{14}N reaction as a source for accelerator-based BNCT, Med. Phys. 28 (2001) 796–803.
[38] R. Uhlář, M. Kadulová, P. Alexa, J. Pištora, A new reflector structure for facility thermalizing D-T neutrons, J. Radioanal. Nucl. Chem. 300 (2014) 809–818.
[39] J.A.G. Gallardo, M.A.N. Giménez, J.L. Gervasoni, Nuclear properties of Tungsten under 14 MeV neutron irradiation for fusion-fission hybrid reactors, Ann. Nucl. Energy 147 (2020) 107739.
[40] N.A.A. Elsheikh, Gamma-ray and neutron shielding features for some fast neutron moderators of interest in ^{252}Cf-based boron neutron capture therapy, Appl. Radiat. Isot. 156 (2020) 109012.
[41] J.P.N. Cárdenas, et al., Experimental and MCNP studies of Paraffin and Polyethylene in neutron moderation and BF_3 detector efficiency, 3rd International Conference on Advancements in Nuclear Instrumentation, Measurement Methods and their Applications (ANIMMA) (2013) 1–5.
[42] X-5 Monte Carlo Team, MCNP-A General Monte Carlo N-Particle Transport Code: Overview and Theory, Los Alamos National Laboratory, 2003. Version 5.
[43] M. Asamoah, et al., Neutron flux distribution in the irradiation channels of Am-Be neutron source irradiation facility, Ann. Nucl. Energy 38 (2011) 1219–1224.
[44] Z. Youxiang, J. Yongli, W. Jimin, The evaluation of cross sections for n+^{6}Li reaction, Communication of Nuclear Data, Progress 28 (2002) 43–45.
[45] Q. Shao, et al., Development and application analysis of high-energy neutron radiation shielding materials from tungsten boron polyethylene, Nucl. Eng. Technol. 56 (2024) 2153–2162.
[46] M. Komárek, V. Ettler, V. Chrastný, M. Mihaljevič, Lead isotopes in environmental sciences: a review, Environ. Int. 34 (2008) 562–577.
[47] T. Schönfeldt, et al., Broad spectrum moderators and advanced reflector filters using ^{208}Pb, Nucl. Instrum. Methods Phys. Res. 769 (2015) 1–4.
[48] A.A. Valter, G.L. Khorasanov, V.E. Storizhko, A.V. Andreev, et al., Investigation of possibilities for production of radiogenic lead highly enriched with 208 Isotope from Thorium ores of Ukraine, in: Proceedings of the Fourth Conference "Heavy Liquid-Metal Coolants in Nuclear Technologies" (HLMC-2013) vol. 2, Obninsk, SSC RF-IPPE V, 2013, pp. 366–372.
[49] G. Mauri, et al., Fast neutron sensitivity for ^{3}He detectors and comparison with Boron-10 based neutron detectors, EPJ Techniques and Instrumentation 6 (2019) 1–22.
[50] A. Tomanin, P. Peerani, G.J. Maenhout, On the optimisation of the use of ^{3}He in radiation portal monitors, Nucl. Instrum. Methods Phys. Res. 700 (2013) 81–85.
[51] S.A. Pozzi, S.D. Clarke, M. Paff, A. Di Fulvio, R.T. Kouzes, Comparative neutron detection efficiency in He-3 proportional counters and liquid scintillators, Nucl. Instrum. Methods Phys. Res. A 929 (2019) 107–112.